The International Journal of Advanced Manufacturing Technology (2018) 97:2667–2674
https://doi.org/10.1007/s00170-018-2111-x

ORIGINAL ARTICLE

Reduction of corner radius of cylindrical parts by magnetic force under various loading methods

Xiaohui Cui[1,2] · Hailiang Yu[1] · Qingshan Wang[1]

Received: 20 July 2017 / Accepted: 4 May 2018 / Published online: 18 May 2018

Abstract

To prevent small corner radius of cylindrical parts from cracking near the sheet bottom corner during deep drawing, a new method combining multidirection magnetic force electromagnetic forming and traditional stamping is proposed in this paper. First, a punch with an 8-mm corner radius is used to obtain a cylindrical part. Then, a coil-generated multidirection magnetic force is used to further deform the sheet corner radius and obtain a smaller corner radius. ANSYS/emag and ABAQUS/explicit software are used to calculate the multiphysical field coupling process in electromagnetic forming (EMF), and obtain accurate simulation data based on the experimental results. We found the following that the maximum thickness thinning ratio was 20% in the sheet corner region with an applied multidirection magnetic force in comparison to 33% if only a bulging coil was used.

Keywords Deep drawing · Electromagnetic combined forming · Multidirection magnetic force · Thickness thinning

1 Introduction

The wall thickness of a workpiece is not evenly distributed in the traditional drawing deep process for a cylindrical part. The main reason for workpiece breaks during the traditional cylindrical deep drawing process is that the tensile stress acting on the part sidewall is larger than the breaking strength. In order to increase the forming depth, the tensile stress should be reduced. Therefore, the hydrodynamic deep drawing method has rapidly developed both home and abroad.

Nakamura et al. [1] proposed a hydraulic counter-pressure deep drawing process assisted by radial pressure. The liquid in the liquid pool is brought to the edge of the sheet blank through a bypass, which can apply a radial pressure to the blank edge to increase the material flow property and significantly improve the sheet rupture resistance. Liu et al. [2] proposed a hydrodynamic deep drawing method combined with an independent radial pressure. When the liquid pressure in the chamber is fixed at 2 MPa, the minimum sheet thickness can be increased from 0.77 to 0.83 mm by increasing the independent liquid pressure from 20 to 35 MPa. However, there are some disadvantages when using the hydro-mechanical deep drawing method in comparison to the traditional stamping process: (1) a larger drawing force and blank-holder force are required, which can increase equipment costs; and (2) sealing is difficult at high pressures.

Electromagnetic forming is a high velocity forming method, which has several advantages in comparison to conventional quasi-static forming processes. These advantages include increased forming limits, reduced spring-back, low tooling costs, and high repeatability [3]. In this process, the coil stays in a fixed position and the sheet metal is deformed in an electric discharge, so one can only manufacture small and shallow parts in a conventional electromagnetic sheet forming process.

To produce deep parts for industrial applications, the electromagnetic-assisted stamping (EMAS) method—which combines traditional deep drawing with electromagnetic forming—has been proposed. For example, Liu et al. [4] used EMAS technology to decrease the corner radius of a cylindrical cup. First, a pre-forming part with an 8-mm corner radius was produced through traditional stamping. Then, a discharge coil was used for an additional deformation of the corner sheet region to produce a 5-mm corner radius. However, it is difficult to greatly increase the forming depth because the method has not yet resolved the problem of material flow in the sheet flange region.

✉ Xiaohui Cui
cuixh622@csu.edu.cn

[1] College of Mechanical and Electrical Engineering, Central South University, Changsha, People's Republic of China

[2] Light alloy research institute, Central South University, Changsha, People's Republic of China

Recently, different researchers [5–9] have placed coils at various sheet/tube metal regions to generate a multidirectional magnetic force on the sheet/tube metal. Cui et al. [5] set up a coil at the end of a sheet to generate a radial magnetic force located in the sheet end, with the radial magnetic force pointed to the die center. This greatly decreases the thickness reduction at the easily broken position and significantly increases the drawing depth of a cylindrical cup. Cui et al. [9] set up a coil at the end of the tube to generate an axial magnetic force located in the tube end. The axial magnetic force pushes the material at the tube end into the bulging region; a larger bulging height can be obtained by improving the feed rate using the axial magnetic pressure even when a smaller discharge voltage is used. However, the above multidirectional magnetic force techniques were only used to increase the drawing depth or bulge height; it cannot be used to manufacture extreme parts with difficult local deformation areas.

Therefore, this paper proposes a new method that combines a radial magnetic force with the EMAS method. ANSYS/emag and ABAQUS/explicit software are used to calculate the multiphysical field coupling process and discusses the effects of different magnetic force loading methods on the cylindrical part radius.

2 EMAS with bulging coil

2.1 Structure field model

Figure 1a shows the geometric model of the forming system. Note that the bulging coils are embedded in the punch corner. A circular aluminum 5052-O sheet of 1 mm in thickness and 96 mm in diameter was used in the experiment. The gap between the blank holder and die was set to 1.12 mm. The corner radius of punch was set to 8 mm, and the die bottom corner radius was set to 5 mm. The numerical simulation conditions are the same with the experimental conditions in Ref. [4]. So, Additional information about this experimental setup can be seen in Ref. [4]. The yield strength of the sheet was 90 MPa. As shown in Ref. [4], the quasi-static constitutive behavior of AA5052-O sheet is described by Eq. (1). To consider the effect of a high strain rate on the forming process, the Johnson-Cook constitutive model should be used in the ABAQUS/explicit finite-element analysis software. The Johnson-Cook (J-C) constitutive model has more accurate predictions of flow stress based on the strain rate induced from 10^{-4} to 10^{4} s^{-1}. Therefore, J-C model was very suitable for electromagnetic forming process [3]. Li et al. [10] used finite-element method to simulate planar and spatial force in the AA5052-O aluminum alloy during mechanical deformation and electromagnetic forming. The J-C constitutive model was also used in the simulation process. Thus, the same strain rate sensitivity coefficient was also used in this paper. The equation contained strain rate effect for 5052-O is shown in Eq. (2).

$$\sigma_s = 364.16\varepsilon^{0.25} \tag{1}$$

$$\sigma = \sigma_s\left(1 + 0.02511\ln\dot{\varepsilon}\right) \tag{2}$$

where σ is the dynamic flow stress, σ_s is the quasi-static flow stress, ε is the plastic strain, and $\dot{\varepsilon}$ is the strain.

The ABAQUS/explicit software was used to establish a two-dimensional (2D) deep drawing model. To increase calculation speed, the punch and die were treated as rigid bodies. Contact conditions between the punch and sheet, as well as the sheet and die, were considered. Coulomb friction law has been used with a friction coefficient of 0.1. During stamping, the punch moves down to draw a cylindrical part 24.5 mm in depth, as shown in Fig. 1a; the simulation time length was set to 10 s. The deformation model was set to axial symmetry,

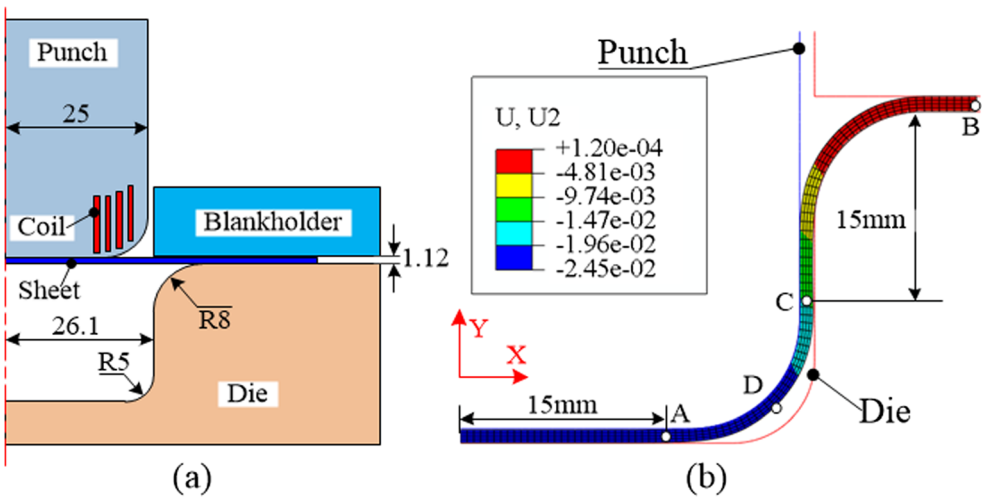

Fig. 1 Structure field model of the (**a**) forming system and (**b**) preforming

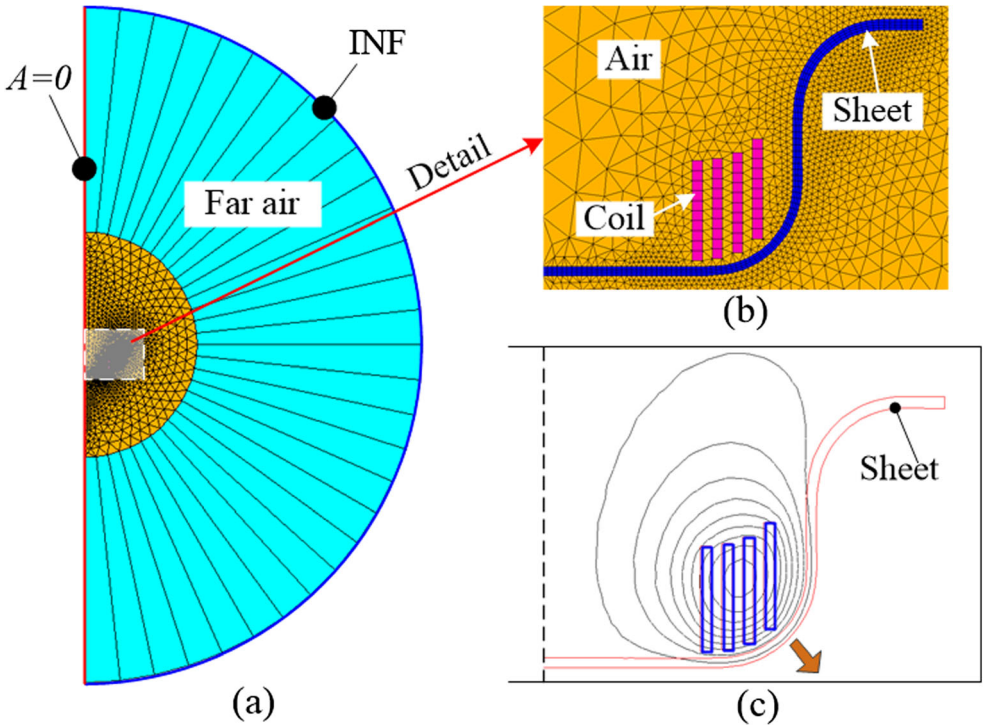

Fig. 2 Electromagnetic field model. **a** Meshing and setting boundary conditions. **b** Detailed region. **c** Distribution of magnetic lines

and the element type for the sheet was set to *CAX4R*. To aid in the follow-up analysis, a rectangular coordinate system was established; special positions on the sheet are defined as points *A*, *B*, *C*, and *D*, as shown in Fig. 1b.

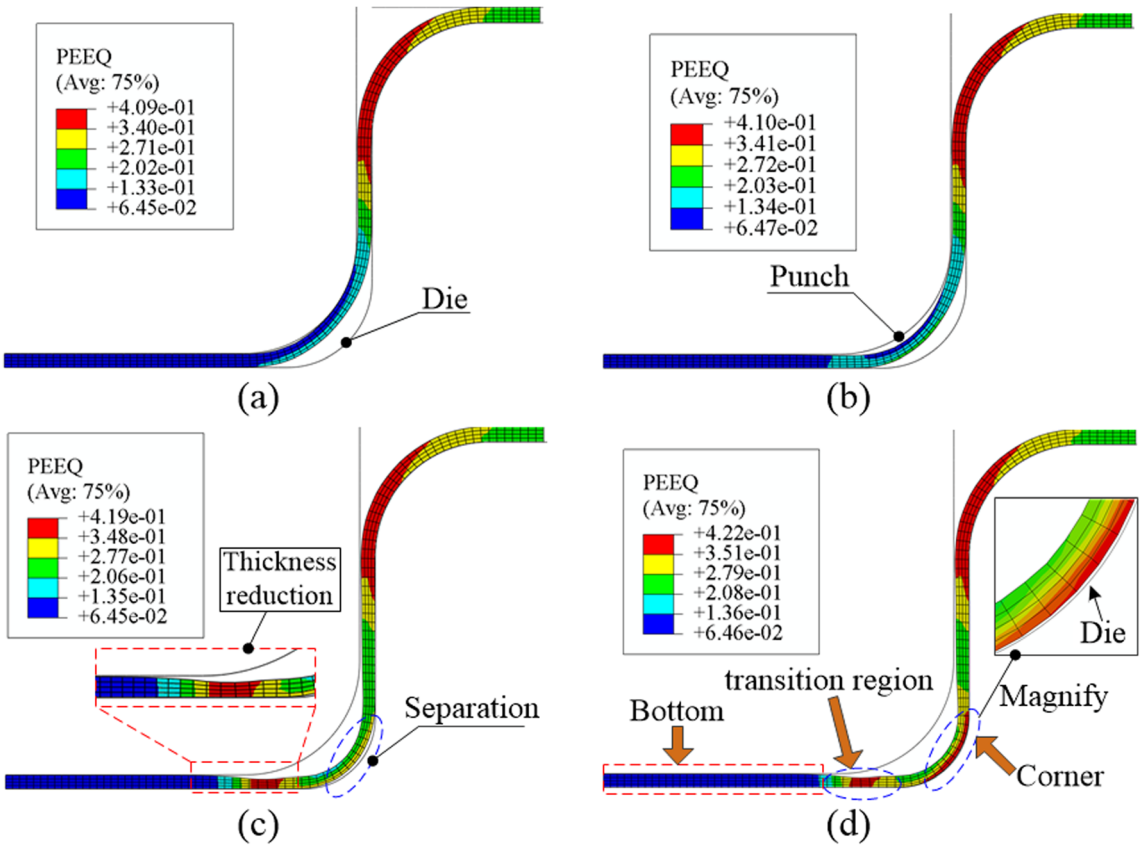

Fig. 3 Changes to equivalent plastic strain for different voltages. **a** 4.5 kV, **b** 5 kV, **c** 5.75 kV, and **d** 6.5 kV

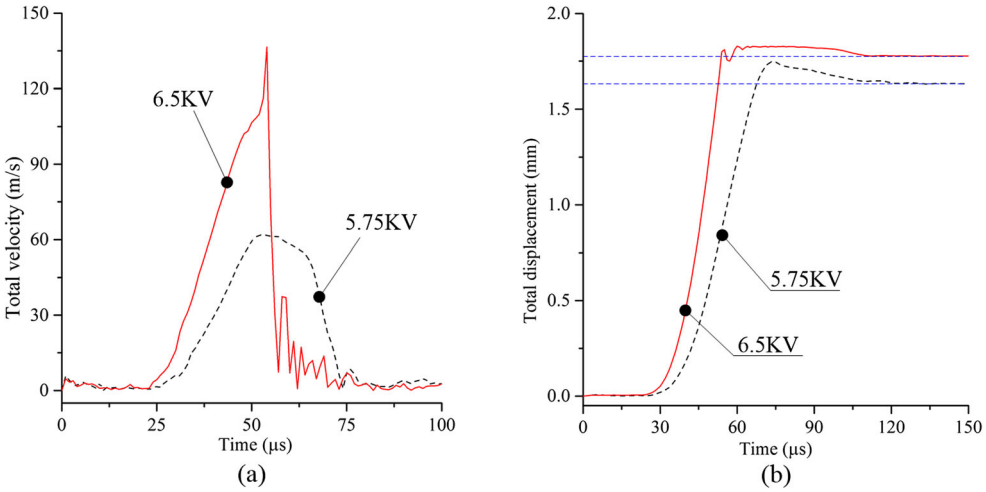

Fig. 4 Deformation results with respect to time at point *D*. **a** Total velocity and **b** total displacement

2.2 Electromagnetic field model

Only half of the forming system was considered in the 2D finite-element (FE) model, as shown in Fig. 2. This is because of the axially symmetric placement of the coil and sheet. The ANSYS/emag software was used to calculate the magnetic force acting on the sheet. The electromagnetic field model consists of a far-air region, an air region, the coils, and the sheet. The sheet and coil were meshed into four-node elements using Plane 13 element types. The air region was meshed into trilateral elements using Plane 13 element types. The far-air region was meshed into four-node elements using Infin 110 element types. The boundary condition was set at the outermost layer of the far-air region (i.e., the magnetic field terminates at the edge of this region). A four-turn spiral coil was used to deform the sheet using magnetic force; the cross-sectional area of the coil is 1 mm × 10 mm.

Figure 2b shows detailed local information about the coil, the air, and the preformed sheet. Thus, the effect of the preformed sheet on the magnetic field calculation is considered in the following analysis. Figure 2c shows the electromagnetic field simulation results based on the deformed sheet. Note that the magnetic lines concentrate near the bottom corner of the sheet.

3 Analysis of simulation results in EMAS with a bulging coil

Figure 3 shows the equivalent plastic strain shift for different discharge voltages. As the discharge voltage increases, the sheet bottom corner moves closer to die bottom corner. If the discharge voltage is less than 5 kV, a small deformation occurs at the sheet bottom corner. If the discharge voltage is larger than 5.75 kV, the sheet bottom corner almost fills the die bottom corner. However, there is always a gap between the sheet bottom corner and the die bottom corner, regardless of the discharge voltage. In addition, both severe plastic deformation and sheet thinning occur at the transitional region between the sheet bottom corner and sheet bottom.

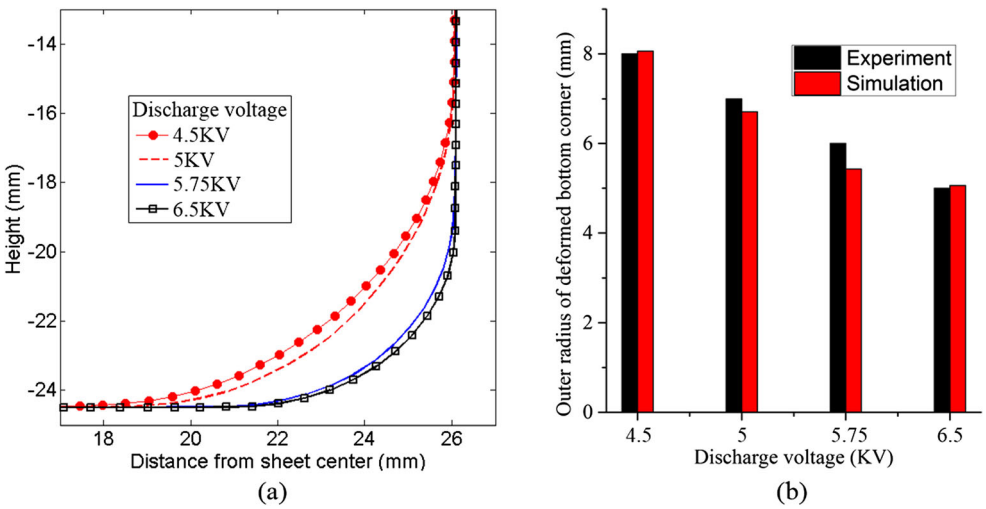

Fig. 5 Deformation results in EMAS. **a** Final profiles for the external corner radius and **b** sheet external corner radius (experiment and simulation)

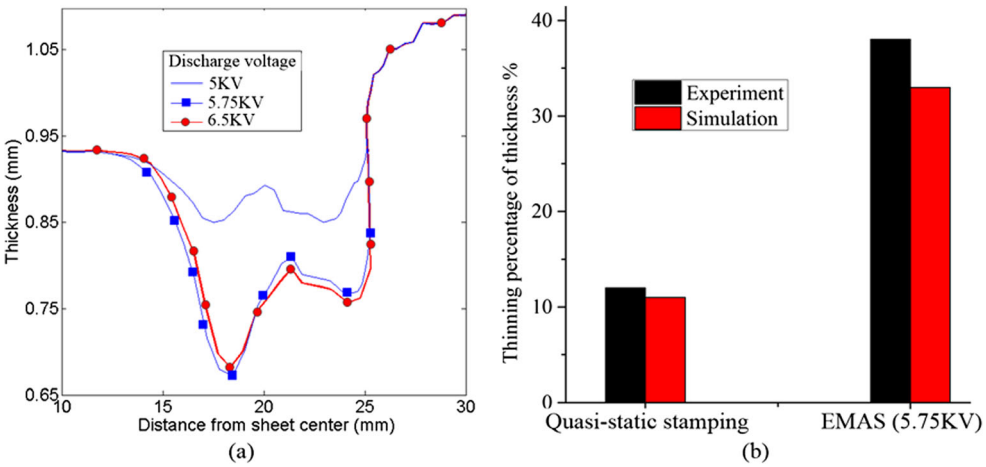

Fig. 6 Thickness distribution for various discharge voltages. **a** Thickness distribution along the sheet bottom corner and **b** maximum thickness reduction

Figure 4a shows the changes of total velocity with time at the *D* point at different voltages. For 5.75 kV, the velocity first increases and reaches a maximum value at roughly 52 μs before gradually decreasing. However, for 6.5 kV, the velocity reaches a maximum value at roughly 55 μs before sharply decreasing. This shows that the sheet corner did not impact the die bottom corner for the 5.75-kV case, but did impact the die at a high speed for the 6.5-kV case. Figure 4b shows the changes of total displacement with time at the *D* point at different voltage. For 6.5 kV, the displacement first increases and then gradually decreases. This is because the sheet corner impacts the die bottom corner, which causes the sheet bottom corner to exhibit a rebound effect. However, for 5.75 kV, the displacement also first increases and then gradually decreases. Based on the results in Fig. 4a, the sheet does not impact with die in the 5.75-kV case. Therefore, the displacement reduction at *D* point in the 5.75-kV case may be caused by the release of

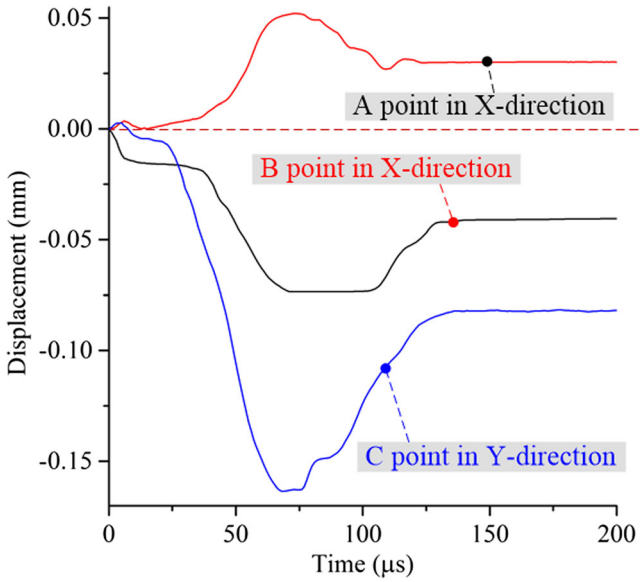

Fig. 7 Changes to displacement with respect to time at special nodes ($U = 5.75$ kV)

elastic waves and plastic waves during the high speed forming process. The final displacement is less than the maximum value for both the 5.75- and 6.5-kV cases, so a gap exists between the sheet bottom corner and the die bottom corner for all discharge voltages.

Three experimental results including corner radius, maximum thickness thinning, and thickness distribution after discharging were shown in Ref. [4]. There exist two obvious regions about thickness reduction according to the thickness distribution with 5.75 kV discharge in simulation, which was coincided with the experimental result. However, the experimental data of thickness distribution was inapplicable to contrast with the simulation result due to inadequate coordinate information in Ref. [4]. Therefore, the corner radius and the maximum thickness thinning after discharge both in experiment and simulation were listed in this paper. Figure 5 shows the deformed sheet profiles obtained by extracting the external profile in Fig. 3. Note that the sheet bottom corner moves closer to the die bottom corner for larger voltages. Figure 5b shows changes to the sheet corner radius in the external profile for different voltages (both experimental and simulated). Note that the simulation method used in this paper accurately predicts the EMAS process results.

Figure 6 shows the thickness distribution along the sheet bottom corner. Note that there are two local necking for the differing discharge voltages. The first thickness reduction is located about 18 mm from the sheet bottom center. Based on the forming system in Fig. 1a, this point corresponds to the transition region between the sheet bottom and the sheet bottom corner. The second thickness reduction is located about 25 mm from the sheet bottom center. Based on the forming system in Fig. 1a, this point corresponds to the transition region between the sheet vertical wall and sheet bottom corner. According to the above analysis, the two areas of greatest thickness reduction are located at both ends of the sheet bottom corner. Figure 6b shows the maximum thickness reduction distribution for both experiment and simulation at

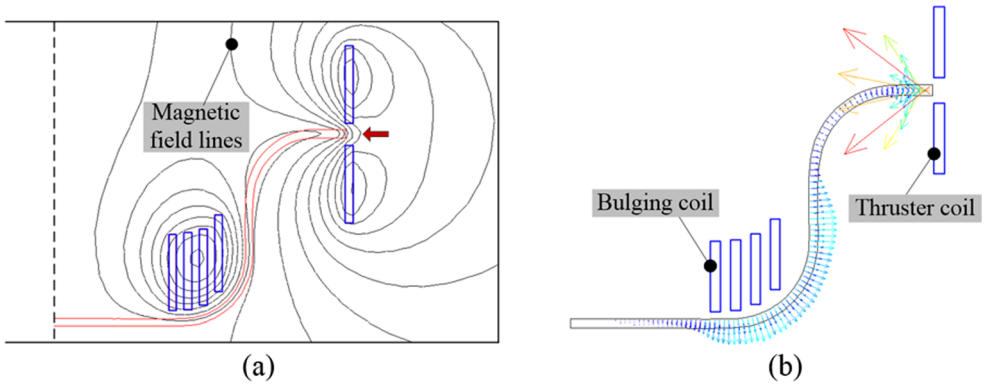

Fig. 8 Magnetic field results for multi-coil discharge. **a** Magnetic flux lines and **b** magnetic force

5.75 kV. Based on the results in Figs. 5b and 6b,, we can conclude that the simulation method used in this paper has a high accuracy in predicting EMAS process results.

In order to rationally explain the thickness distribution after coil discharge, it is necessary to understand the laws governing material plastic flow during the forming process. Figure 7 shows the changes to displacement over time along the *X* axis at points *A* and *B*, and the displacement along the *Y* axis at point *C*. The displacement at point *A* increases by 0.025 mm. The displacement at point *B* is larger than the one at point *A*, which causes a larger plastic flow at point *C* along the *Y* axis due to the materials at sheet flange moves to die hole. A more severe thickness reduction appears at point *A* than at point *C*, because the displacement at point *C* is larger than at point *A*. However, the displacements at points *A*, *B*, and *C* are all very small, which causes the materials at the sheet bottom corner to form a bulge.

4 EMAS with multidirection magnetic force

In order to reduce the severe thickness reduction at the sheet bottom corner after coil discharge, it is necessary to find a way to make the materials at the sheet bottom and the sheet vertical wall flow to the sheet bottom corner. Based on this need, we propose adding a thruster coil at the sheet end. The cross-section of the thruster coil is 1 mm × 10 mm. The magnetic flux lines after the bulging and thruster coils discharge can be seen in Fig. 8a. Note that the electromagnetic field is concentrated at the sheet end and the sheet bottom corner, which generates multidirection magnetic forces in different regions of the sheet, as shown in Fig. 8b.

Figure 9 shows the final deformation results for coil discharges at 5.75 and 6.5 kV. Note that the sheet bottom corner contacts and perfectly fits with die bottom corner no matter the discharge voltage. From an equivalent plasticity strain view, the sheet bottom corner and its surrounding area did experience a large plastic strain and small thickness thinned. Compared to the 5.75-kV results, the 6.5-kV example had a larger radial magnetic force acting on sheet end, which caused more material to flow from the sheet flange to the die hole. A small bump appears at sheet upper corner in the 6.5-kV sample, because the sheet upper corner is not clamped by a blank holder.

Figure 10 shows the displacement change with respect to time along the *X* axis at points *A* and *B*, and along the *Y* axial at point *C* when the two coils both discharge. Note the following: (1) almost no material flows at point *A*; (2) and there is a larger material flows at points *B* and *C* in comparison to the results from Fig. 7, which will cause a smaller thickness

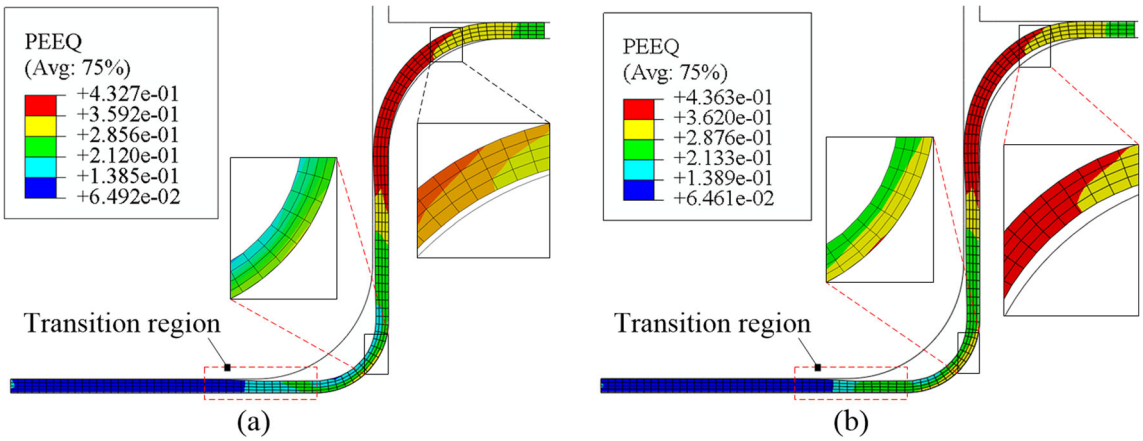

Fig. 9 Deformation results for multi-coil discharges at **a** 5.75 kV and **b** 6.5 kV

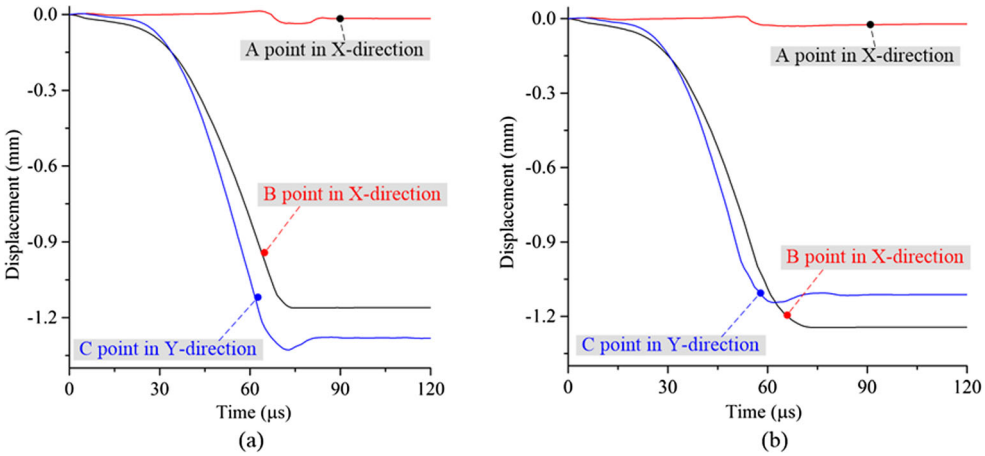

Fig. 10 Displacement change with respect to time in response to multidirection magnetic force. **a** 5.75 kV and **b** 6.5 kV

reduction at the sheet bottom corner. Compared to the results for 5.75 kV, the 6.5-kV sample has a larger displacement at point *B* and a smaller displacement at point *C*. The small displacement at point *C* indicates a smaller material flow from the sheet vertical wall to the sheet bottom corner, and there is a greater thickness reduction at the sheet bottom corner.

Based on the sheet deformed shapes in Fig. 9, the thickness distribution after discharging two coils can be seen in Fig. 11. Note that the maximum thickness reduction in the 6.5-kV sample is larger than the one for the 5.75-kV sample. This is due to the larger magnetic force on the sheet end; a bigger bulge appears at the sheet upper corner, which hinders the material flow from the sheet flange to the sheet bottom corner. For the 5.75-kV sample, the maximum thickness reduction is about 20% using multi-coil discharge in comparison to a maximum thickness reduction of about 33% using the bulging coil in Fig. 6.

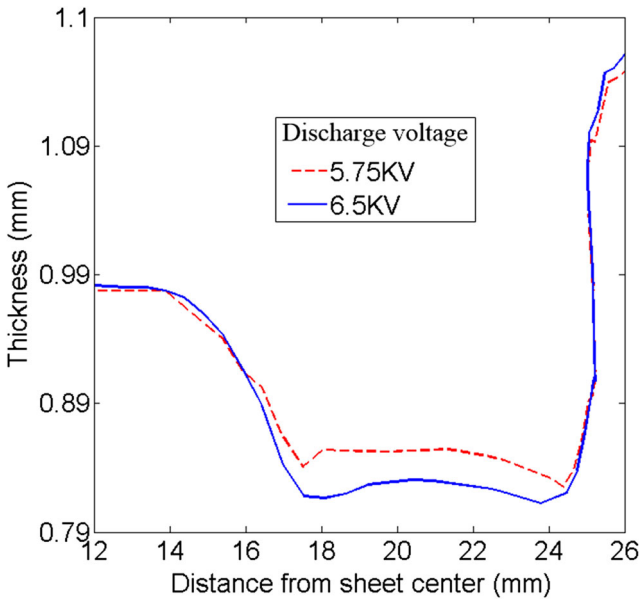

Fig. 11 Thickness distribution using multi-coil discharge

5 Conclusion

(1) The sheet bottom corner does not contact or fit the die bottom corner when using a bulging coil, no matter the discharge voltage. There are two distinct areas of sheet thinning. Based on the experimental results, the simulation method used in this paper accurately predicts the results of the EMAS process.

(2) The material fluidity at the sheet flange and the sheet vertical wall have been significantly improved by using two coil discharge, which results in a more uniform thickness at the sheet bottom corner. The maximum thickness reduction is reduced from 33 to 20% after using two coil discharges in comparison to using just a bulging coil.

Funding information This work was supported by the National Natural Science Foundation of China (Grant Nos. 51775563 and 51405173), State Key Laboratory of Materials Processing and Die & Mould Technology, Huazhong University of Science and Technology (No. P2017-013) and the Project of State Key Laboratory of High Performance Complex Manufacturing, Central South University (ZZYJKT2017-03) and Guangzhou Science and Technology Plan Project (201707010472).

References

1. Nakamura K, Nakagawa T (1987) Sheet metal forming with hydraulic counter pressure in Japan, CIRP Annals- Manufacturing Technol. 36(1):191–194
2. Liu XJ, Cong YL, Li F, Xu YC, Yuan SJ (2010) Effect of independent radial pressure loading paths on cup thickness distribution. J Central South University (Sci Technol) 41:917–922
3. Psyk V, Risch D, Kinsey BL, Tekkaya AE, Kleiner M (2011) Electromagnetic forming—a review. J Mater Process Technol 211:787–829

4. Liu DH, Li CF, Yu HP (2009) Numerical modeling and deformation analysis for electromagnetically assisted deep drawing of AA5052 sheet. Trans Nonferrous Met Soc China 19:1294–1302
5. Cui XH, Li JJ, Mo JH, Fang JX, Zhou B, Xiao XT, Feng F (2016) Incremental electromagnetic-assisted stamping (IEMAS) with radial magnetic pressure: a novel deep drawing method for forming aluminum alloy sheets. J Mater Process Technol 233:79–88
6. Cui XH, Mo JH, Fang JX, Li JJ (2014) Deep drawing of cylindrical cup using incremental electromagnetic assisted stamping with radial magnetic pressure. Procedia Engineering 81:813–818
7. Fang JX, Mo JH, Cui XH, Li JJ, Zhou B (2016) Electromagnetic pulse-assisted incremental drawing of aluminum cylindrical cup. J Mater Process Technol 238:395–408
8. Lai ZP, Cao QL, Zhang CB, Han XT, Zhou ZY, Xiong Q, Zhang X, Chen Q, Li L (2015) Radial Lorentz force augmented deep drawing for large drawing ratio using a novel dual-coil electromagnetic forming system. J Mater Process Technol 222:13–20
9. Cui XH, Mo JH, Li JJ, Xiao XT (2017) Tube bulging process using multidirectional magnetic pressure. Int J Adv Manuf Technol 90(5–8):2075–2082
10. Li N, Yu HP, Xu Z, Fan ZS, Liu L (2016) Electromagnetic forming facilitates the transition of deformation mechanism in 5052 aluminum alloy. Mater Sci Eng A 673:222–232